Interstellar Plasma Scattering Effects Studied with Radioastron

© **A. Andrianov**[1], **M. V. Popov**[1], **N. Bartel**[3], **H. Bignall**[4], **C. Gwinn**[5], **M. Johnson**[6], **D. Jauncey**[7], **E. Fadeef**[1], **B. Ch. Joshi**[8], **N. Kardashev**[1], **R. Karuppusamy**[9], **Yu. Y. Kovalev**[1], **M. Kramer**[9], **A. Rudnitskiy**[1], **V. Shishov**[2], **T. Smirnova**[2], **V. A. Soglasnov**[1], **A. Zensus**[9]

[1]The Astro Space Center of Lebedev Physical Institute of RAS, Moscow, Russia
[2]Pushchino Radio Astronomy Observatory, Astro Space Center, Lebedev Physical Institute of RAS, Moscow, Russia
[3]York University, Toronto, Canada
[4]Curtin University of Technology, Perth, Australia
[5]University of California at Santa Barbara, Santa Barbara, USA
[6]Harvard-Smithsonian Center for Astrophysics, Cambridge, USA
[7]CSIRO Astronomy and Space Sciences, Epping, Australia
[8]National Centre for Radio Astrophysics, Pune, India
[9]Max Planck Institute for Radio Astronomy, Bonn, Germany

On behalf of the Radioastron pulsar group this report presents an overview of the studies which were done with the Radioastron space radio telescope during the first five years of mission operation, including the early and key science programs. Space-VLBI observations of pulsars with the highest angular resolution revealed the new interstellar plasma scattering effects, such as resolved substructure in the scattering disk. Diameters of the scattering disks were measured for several pulsars and the distances to the effective scattering screens were estimated. For close pulsars the layers of scattering plasma were detected to be located relatively close to the Sun (0.17–100 pc). Such layers might be responsible for fast flux variations of compact extragalactic radio sources. A new insight on the interstellar scattering was demonstrated by study of the instantaneous visibilities which were measured with the Space-VLBI observations of giant pulses from the Crab pulsar.

Keywords: VLBI, Radioastron, Pulsars, Interstellar medium.

1 PSR 0329+54

Fine structure in the scattering disk of PSR B0329+54 was discovered in observations with Radioastron space-ground interferometer at baseline projections from

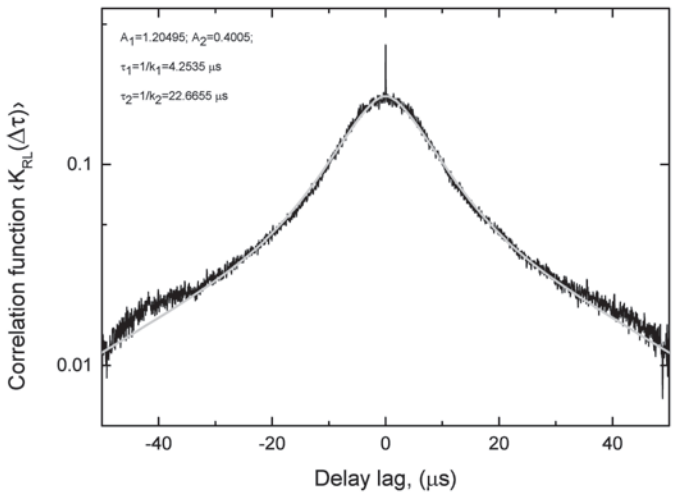

Fig. 1. Example of cross-correlation function KRL($\delta\tau$) averaged over 570 seconds. Solid gray line corresponds to two-exponential fit

60,000 km to 235,000 km. Observations were performed at 324 MHz with the support of 110-m Green Bank Telescope during four days in November 2012. Interferometric visibility at such long baselines has random variations of phase and amplitude. Visibility function has a localized, extended region around the origin, composed of many random spikes. We analyzed a cross-correlation between squared modulus of visibility obtained in two polarization channels (LCP and RCP). Example of such cross-correlation function is shown in Fig. 1. One can see that there are two time scales in the CCF. We argue theoretically that such shape may be given by the average envelope of the impulse-response function of interstellar scattering, that has two different exponential scales. Grey solid line in Fig. 1 shows two-exponential fit.

2 Four distant pulsars

We investigated the distribution of scattering plasma in the direction to the four pulsars: B0329+54, B1641-45, B1749-28 and B1933+16, which are located in different regions of the Galaxy. Angular diameters of scattering disks were measured using the visibility amplitude versus baseline distribution. Pulse time broadening was estimated by analyzing visibility function structure along delay coordinate. Distances to the effective scattering screens were estimated through computation of angular and time broadening. The list of obtained scattering parameters is shown in the Table 1. Model of uniform distribution of scattering plasma does not suit to any of the pulsar. For several pulsars the detected scattering layers of plasma

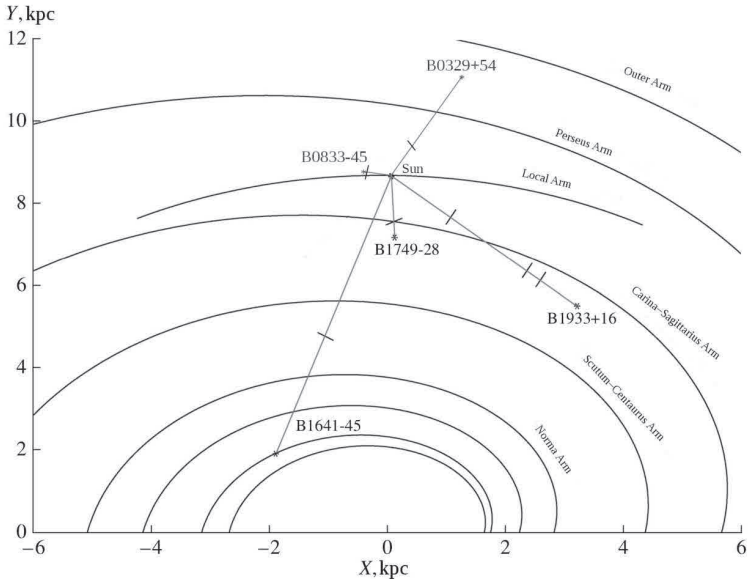

Fig. 2. Location of observed pulsars and scattering screens in the Galactic plane

were identified with astronomical objects such as G339.1-04 (PSR B1641-45) and G0.55-0.85 (PSR B1749-28). The locations of pulsars and scattering screens are shown at Fig. 2.

3 PSR B1641-45

Observation session for PSR B1641-45 lasted 15 hours. Such duration of the observing session provided a good (u,v)-coverage, so that we were able to map the scattering disk. Synthesized image was obtained with Astro Space Locator software package. Relative sensitivity of antennas were estimated from pulsar signal level increment. The scattering disk size was approximated by two-dimensional Gaussian with FWHM 20.6×27.5 mas along right accession and declination respectively. This value is in a good agreement with distribution obtained from using the dependence of visibility vs a baseline projection.

4 Substructure in Scattering Disk of Crab pulsar

Radioastron results showed that Space-VLBI observations with high angular resolution provided an opportunity to resolve the substructure in the scattering disk of the Crab pulsar. Scattering time and distance to the scattering screen are changing from epoch to epoch. For epochs with strong scattering the screen was located close to the Crab Nebula. This indicates the dominant influence of the Crab Nebula on the scattering of the Crab pulsar radio emission.

5 PSR B0834+06

Observations of pulsar B0834+06 were conducted on 08.04.2015 at 324 MHz together with RadioAstron space radio telescope and the large ground radio telescopes Arecibo, Green Bank, Westerbork. Additionally, we analyzed two days of BSA radio telescope observations (02.02.2012 and 04.02.2012) of this pulsar at 112 MHz. We determined frequency and time scintillation scales at 324 MHz ($f_{dif} = 208$ kHz and $t_{dif} = 200$ sec) and at 112 MHz ($f_{dif} = 2$ kHz and $t_{dif} = 40$ sec). Obtained scintillation scales at these two frequencies are in good agreement with each other and coincide with previously published data. Secondary spectrum shows parabolic arcs, which indicate the presence of scattering screens. Distance from the observer to the scattering screen, estimated from parabolic arc curvature, changed from 415 pc in 2005 to 518 pc in 2015.

6 Studies of the Nearby, Turbulent Interstellar Plasma

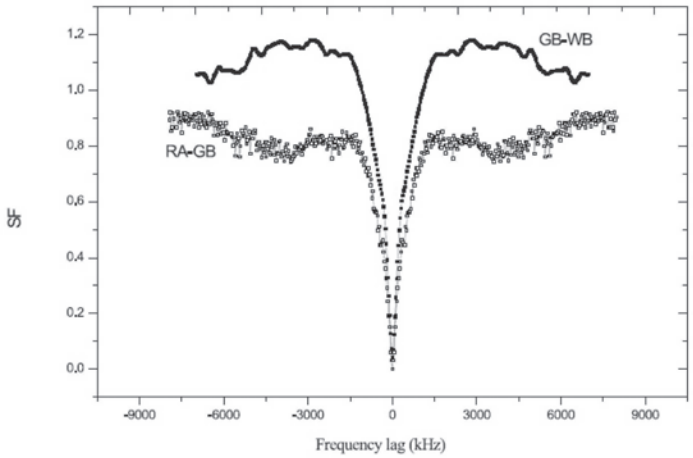

Fig. 3. Normalized frequency structure functions for ground (GB-WB) and space-ground (RA-GB) baselines

Fig. 3 shows averaged frequency structure functions for ground (squares) and space-ground (circles) baselines at zero time lag. Evidently the levels of the structure function (SF) differ by ~ 0.2. This corresponds to the relative contribution of two frequency scales in the scintillation spectra. The ratio of their amplitudes is consistent with the fitting the sum of two exponents into the average frequency correlation function for the ground baseline. The space-ground baseline shows no break in the structure function. This structure function displays the small-scale component of the spectra, with a relative amplitude of 0.8. For pulsars 0950+08 and 0525+21 similar analysis was performed. All results are shown in Table 2.

Table 1

Measured scattering parameters

Pulsar	N_{ch}	δt, (s)	ΔT, (s)	Δt_{sc}, (s)	$\Delta\nu_{d}$, (kHz)	τ_{sc}, (μs)	θ_{H}, (mas)	*l, b,* (°)	D, (kpc)	d, (kpc)
B1641-45	16384	0.45	115	0.20 (0.05)	0.062 (0.002)	2600 (100)	27 (5)	339.2, -0.2	4.9	3.0
B1749-28	256	5.62	225	220 (20)	410 (100)	310 (0.040)	0.5 (0.2)	1.54, -0.96	1.3	0.95
B1933+16	8192	0.35	250	–	0.25 (0.15)	600 (400)	12.3 (0.6)	52.4, -2.1	3.7	2.6
B1933+16	2048	0.35	250	41.6 (0.5)	50.4 (1.1)	3.2 (0.1)	0.84 (0.04)	52.4, -2.1	3.7	2.7 [1.3; 3.1]
B0329+54	2048	0.71	70	102	7 (2)	12 (3)	4.8 (0.8)	145 -1.2	1.0	0.5
B0834+06	65536	1.2	-	200	208	-	-	219.72 , 26.27	0.64	0.512

Table 2

Structure of interstellar plasma in direction to pulsars B0950+08, B1919+21 and B0525+21

	1919+21	0950+08	0525+21
r_{dif}	4.6 *109 cm	1.4-2.7 ·1010cm	2.1 *109 cm
Scattering angle θ_{dif}	0.7 mas	0.33-0.64 mas	0.028 mas
Scintillation time **t**	290 s	1000 s	160 s
z_1	440 pc	26-170 pc	1440 pc
z_2	0.17 pc	4.4-16.4 pc	-
D	1 kpc	262 pc	1.6 kpc
θ_{ref}	150 mas	1.1-4.4 mas	-
Z_{pr}	<= 1 pc	-	-
	**	*	***

* Results published at ApJ — Smirnova et al. 2014, ApJ, 786,115

** Publication is submitted to MNRAS

*** Publication is submitted to Astronomy Reports